region of the Fermi surface, is flat. The low value for $N(0)$[4] and the fact the Cr has a local moment in this class of materials[4,11] imply that the hybridization is probably s-p.

[11] R. H. Willens and E. Buehler, J. Appl. Phys. **38**, 405 (1967).

ACKNOWLEDGMENTS

The authors would like to thank T. H. Geballe and J. H. Wernick for helpful discussions, and also E. Berry for experimental assistance.

PHYSICAL REVIEW VOLUME 159, NUMBER 2 10 JULY 1967

The Mixed State of Thin Superconducting Films in Perpendicular Fields

Alexander L. Fetter*

Institute of Theoretical Physics, Department of Physics, Stanford University, Stanford, California

AND

P. C. Hohenberg

Bell Telephone Laboratories, Murray Hill, New Jersey

(Received 31 January 1967)

The behavior of ideal thin superconducting films in perpendicular magnetic fields is studied in detail and related to that of bulk type-II superconductors. A macroscopic analysis based only on the demagnetizing factors yields the dominant effects of sample geometry on the reversible magnetization curve. The same features are also derived from Pearl's generalization of Abrikosov's microscopic model, which predicts a long-range interaction between quantized flux lines in a thin film. Comparison of the macroscopic and microscopic arguments clarifies some inaccuracies in the work of Pearl and of Maki. The dependence of critical magnetic fields on film thickness is discussed for different values of the Ginzburg-Landau parameter κ. A hydrodynamic calculation demonstrates that a triangular vortex lattice is stable against small perturbations in the long-wavelength limit ($qn^{-1/2}\ll 1$); for $n^{1/2}\Lambda\gg 1$, the corresponding dispersion relation is $\omega=\frac{1}{4}(eB/mc)q^{3/2}\Lambda^{1/2}(n\pi)^{-1/2}$, where n is the vortex density, $\Lambda\equiv 2\lambda^2/d$ is the "effective penetration depth," λ is the actual penetration depth, and $d(\ll\lambda)$ is the film thickness. This conclusion disagrees with Pearl's conjecture based on elasticity theory; the long-range interaction precludes the use of elasticity theory, as is seen from the difference between the calculated dispersion relation ($\omega\propto q^{3/2}$) and that predicted for elastic modes ($\omega\propto q^2$). The dynamics of vortex systems is contrasted with the Newtonian dynamics of point masses. In practice, thin films exhibit highly irreversible behavior, and no detailed comparison between theory and experiment is attempted.

I. INTRODUCTION

It was first pointed out by Tinkham[1,2] that thin superconducting films in perpendicular magnetic fields would exhibit a mixed-state structure analogous to the Abrikosov state,[3] even if the κ value of the film was less than $1/\sqrt{2}$. Subsequently, Pearl[4–6] and Maki[7] adapted the Abrikosov theory to this geometry in a detailed and quantitative way. In an important but only partially published study,[8] Pearl[4–6] observed that the distinctive properties of thin-film vortices arise from their long-range electromagnetic interactions: vortices in a thin film interact primarily through the free space adjacent to the film, where no screening currents can flow. As one consequence of this long-range interaction, Pearl suggested that the vortex lattice, predicted by Abrikosov and experimentally verified in bulk systems,[9,10] would not occur in thin films, since "the shear modulus vanishes."[11] Pearl's work is based entirely on a picture of individual vortices interacting in pairs, which ceases to be valid as the applied magnetic field is increased and the vortices become dense. In the limit $H\lesssim H_{c2}$, near the upper critical field, the free energy may be expanded directly[3,12] in powers of the order parameter, which allows a comparison of various vortex configurations. This approach has recently been extended by Lasher,[13] who showed that

* Research sponsored by the Air Force Office of Scientific Research, Office of Aerospace Research, U. S. Air Force, under AFOSR contract AF49(638)1389.

[1] M. Tinkham, Phys. Rev. **129**, 2413 (1963).

[2] M. Tinkham, Rev. Mod. Phys. **36**, 268 (1964).

[3] A. A. Abrikosov, Zh. Eksperim. i Teor. Fiz. **32**, 1442 (1957) [English transl.: Soviet Phys.—JETP **5**, 1174 (1957)].

[4] J. Pearl, *Low Temperature Physics LT9*, edited by J. G. Daunt, D. O. Edwards, F. J. Milford, and M. Yaqub (Plenum Press, Inc., New York, 1965), Part A, p. 566.

[5] J. Pearl, Appl. Phys. Letters **5**, 65 (1964).

[6] J. Pearl, thesis, Polytechnic Institute of Brooklyn, 1965 (unpublished).

[7] K. Maki, Ann. Phys. (N.Y.) **34**, 363 (1965).

[8] P. G. de Gennes, *Superconductivity of Metals and Alloys* (W. A. Benjamin, Inc., New York, 1966), p. 60.

[9] D. Cribier, B. Jacrot, L. M. Rao, and B. Farnoux, Phys. Letters **9**, 106 (1964).

[10] W. Fite, II, and A. G. Redfield, Phys. Rev. Letters **17**, 381 (1966).

[11] Reference 6, p. 99.

[12] W. H. Kleiner, L. M. Roth, and S. H. Autler, Phys. Rev. **133**, A1226 (1964).

[13] G. Lasher, Phys. Rev. **154**, 345 (1967).

for sufficiently thin films the triangular array had a lower free energy than the other simple lattices (square and honeycomb). Of course, this calculation does not prove the stability of the triangular lattice with respect to small perturbations (which is presumably what Pearl had in mind) or at lower fields $H \ll H_{c2}$.

In this paper, we study the stability of a vortex lattice in thin films on the basis of a hydrodynamical model that was used previously[14] to study the corresponding problem in bulk samples. A stability criterion is formulated for the long-range interaction derived by Pearl; the vibration frequencies are then evaluated both in a continuum approximation, and for a triangular lattice. In each case, the frequencies are real in the long-wavelength limit, which indicates microscopic stability. Hence, the long-range interaction does not automatically destroy the lattice order, in contradiction to Pearl's conjecture. The long-range forces do preclude the use of an elasticity theory, however, since the vibration frequencies here vary as $q^{3/2}$ in contrast to the q^2 dependence of bulk samples.

In Sec. II, the reversible magnetization curve of thin films is analyzed, using only the macroscopic demagnetizing effects, leaving the *constitutive relation* $[\mathbf{B}=\mathbf{B}(\mathbf{H})]$ unchanged. This analysis accounts for the dominant modification of the Abrikosov[3] magnetization curve, namely, that of order R/d,[15] which has not been calculated consistently by previous authors.[4,7] In Sec. III we review the properties of individual vortices in thin films and indicate how these lead to the magnetization curves derived in Sec. II. A qualitative discussion of the dependence of the critical fields on film thickness is given in Sec. IV, along with a review of detailed calculations by other authors. In Sec. V, the hydrodynamic calculation for the vortex lattice demonstrates that the triangular structure is stable in the long-wavelength limit. The dependence of the lattice structure on film thickness and magnetic field is also discussed. Section VI contains a study of the effects arising from the long-range interaction, with particular emphasis on the failure of elasticity theory.

Unfortunately, the magnetization curves of available films are highly irreversible,[16] so that we shall not attempt any detailed comparison with experimental data. We shall see, however, that the theoretical slope of the (reversible) magnetization curve near H_{c2} is even smaller than that predicted by Maki,[7] which was already smaller than the experimental slope by a factor of 10^2–10^3. No experimental evidence of lattice order or indeed of vortex structure in thin films has yet been presented. Nevertheless, we expect that the periodic variation of the magnetic field should be observable, if some method can be found to come close enough to the surface of a uniform film. The lattice vibrations would probably be even more difficult to detect than in bulk materials, where no modes with $\mathbf{q}$ perpendicular to $\mathbf{H}$ have yet been reported.

[14] A. L. Fetter, P. C. Hohenberg, and P. Pincus, Phys. Rev. **147**, 140 (1966), referred to in what follows as I.

[15] d is the film thickness and R is a typical transverse dimension.

[16] G. K. Chang, T. Kinsel, and B. Serin, Phys. Letters **5**, 11 (1963); P. B. Miller, B. W. Kington, and D. J. Quinn, Rev. Mod. Phys. **36**, 70 (1964); cf. also Ref. 2.

II. MACROSCOPIC DESCRIPTION

In this section we shall show that the main difference between the magnetization curves of thin films and bulk type-II materials can be understood with simple macroscopic arguments. The effects are large, of order R/d, where d is the thickness of the film and R a typical dimension perpendicular to d. Consider the magnetization curve of a spheroid of revolution of radius R and height d, in an external magnetic field $\mathbf{H}_0$ pointing along the symmetry axis. The *constitutive relation* $[\mathbf{B}=\mathbf{B}_e(\mathbf{H})]$ is assumed for the moment to be the one derived by Abrikosov[3] for bulk type-II materials, and the magnitude of the field $\mathbf{H}$ is related to the applied field H_0 by the equation

$$H=H_0-4\pi\mathfrak{n}M=H_0-\mathfrak{n}(B-H)=(H_0-\mathfrak{n}B)/(1-\mathfrak{n}), \tag{1}$$

where the demagnetizing factor[17] $\mathfrak{n}$ depends on the ratio R/d. Only the following limiting values are of interest here:

$$\begin{aligned}\mathfrak{n}&=1-(\pi/2)(d/R) && \text{for } d/R\ll 1 \text{ (flat disk)},\\ \mathfrak{n}&=(R/d)^2\ln(d/R) && \text{for } R/d\ll 1 \text{ (long cylinder)}.\end{aligned} \tag{2}$$

If Eq. (1) is inserted into the constitutive relation, we obtain the implicit equation[18]

$$B=B_e[(H_0-\mathfrak{n}B)/(1-\mathfrak{n})]. \tag{3}$$

Equation (3) requires that B vanish until H_0 reaches the value

$$H_{c1}^0=(1-\mathfrak{n})H_{c1}, \tag{4}$$

which behaves like d/R for the flat disk. Furthermore when M goes to zero, the fields H, H_0, and B all become equal, so that $H_{c2}^0=H_{c2}$ is independent of $\mathfrak{n}$. The magnetization curve of M versus H_0 has the shape indicated in Fig. 1(b) and depends sensitively on the ratio d/R, in contrast to the Abrikosov curve $M(H)$, represented in Fig. 1(a).

The area under the magnetization curve is independent of the shape of the sample, however, which can be seen from the following derivation[19]: Equation

[17] See, for example, L. D. Landau and E. M. Lifshitz, *Electrodynamics of Continuous Media* (Pergamon Press, Ltd., London, 1960).

[18] Cf. Ref. 8, p. 74. We warn the reader that there is an unfortunate misprint in Ref. 8; the correct equation is clearly our Eq. (3).

[19] See also I. O. Kulik, JETP Pis'ma Redaktsiyu **3**, 398 (1966) [English transl.: Soviet Phys.—JETP Letters **3**, 259 (1966)]. See also J. A. Cape and J. M. Zimmerman, Phys. Rev. **153**, 416 (1967).

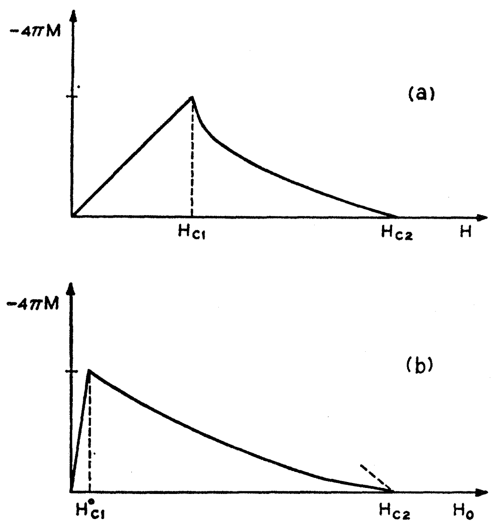

FIG. 1. (a) The Abrikosov magnetization curve $-4\pi M$ versus H. (b) The magnetization curve $-4\pi M$ versus H_0 for a flat disk with $d/R \ll 1$.

(1) is an implicit relation for H_0 as a function of H. If we define

$$M(H_0(H)) \equiv M_e(H) = [B_e(H) - H]/4\pi, \qquad (5)$$

then

$$dH_0 = dH(1 + 4\pi\mathfrak{n}(dM_e/dH)). \qquad (6)$$

The area under the magnetization curve is given by

$$\begin{aligned}\int_0^{H_{c2}} M(H_0)\,dH_0 &= \int_0^{H_{c2}} M_e(H)(1+4\pi\mathfrak{n}(dM_e/dH))dH \\ &= \int_0^{H_{c2}} M_e(H)\,dH + 2\pi\mathfrak{n}[M_e^2(H_{c2}) - M_e^2(0)] \\ &= \int_0^{H_{c2}} M_e(H)\,dH, \end{aligned} \qquad (7)$$

which is therefore independent of the demagnetizing coefficient $\mathfrak{n}$.

The slope of the magnetization can be found by differentiating Eq. (3) and using Eq. (5). An elementary calculation shows that

$$-4\pi \frac{dM}{dH_0} = -\frac{4\pi(dM_e/dH)}{1+4\pi\mathfrak{n}(dM_e/dH)}. \qquad (8)$$

In a long thin cylinder where $\mathfrak{n}=0$ and $H=H_0$, we recover Abrikosov's result[3] which predicts that $4\pi dM/dH$ is infinite for H just above H_{c1}, and is a finite constant at H_{c2}. For any other geometry ($\mathfrak{n}\neq 0$, $H\neq H_0$) the slope $4\pi dM/dH_0$ is finite and equal to $1/\mathfrak{n}$ for H_0 just above H_{c1}^0. At H_{c2}, the slope $4\pi dM/dH_0$ is necessarily less than $1/\mathfrak{n}$. For a flat disk, where $\mathfrak{n}$ is one [minus corrections of order d/R, Eq. (2)], this result leads to the prediction that near H_{c2}, the *reversible* curve of $-4\pi M$ versus H_0 always lies below the straight line with slope minus one, independent of the exact form of $M(H)$. It is shown below (Sec. III) that these predictions cannot be derived immediately from the microscopic theory and have been misstated in previous treatments.[4,7]

III. MICROSCOPIC DESCRIPTION

We shall first review Pearl's[6] solution of the Ginzburg-Landau equations for a single vortex in a thin film. The basic dimensionless parameter, which we temporarily assume to be small, is the ratio of the thickness d to the penetration depth λ. The film lies in the x-y plane with the vortex at the origin. In the narrow-core approximation (whose validity will be discussed in Sec. IV) the order parameter has the form

$$\begin{aligned}\Psi(\mathbf{r},z) &= \Psi_0 \exp(i\theta) \qquad |z|<d/2 \\ \Psi(\mathbf{r},z) &= 0 \qquad |z|>d/2,\end{aligned} \qquad (9)$$

where $\mathbf{r}$ is a two-dimensional vector in the x-y plane with polar coordinates (r,θ) and the spatial variation of Ψ_0 is neglected. If the external magnetic field $\mathbf{H}_0$ is in the z direction, the vector potential satisfies the equation

$$\begin{aligned}\nabla\times\nabla\times\mathbf{A} &= \frac{4\pi}{c}\mathbf{j}_s = \frac{1}{\lambda^2}\left[\frac{\hat{\theta}\varphi_0}{2\pi r} - \mathbf{A}\right], \qquad |z|<d/2 \\ \nabla\times\nabla\times\mathbf{A} &= 0, \qquad |z|>d/2.\end{aligned} \qquad (10)$$

Since d/λ is assumed small, $\mathbf{j}_s$ and $\mathbf{A}$ are constant across the film, and we can average Eqs. (10) over the thickness d, obtaining

$$\nabla\times\nabla\times\mathbf{A} = \frac{d\delta(z)}{\lambda^2}\left[\frac{\hat{\theta}\varphi_0}{2\pi r} - \mathbf{A}\right]. \qquad (11)$$

The circular symmetry of the problem shows that

$$\mathbf{A}(r,\theta,z) = \hat{\theta} f(r,z), \qquad (12)$$

which leads to an equation for the scalar function f

$$\begin{aligned}\frac{\partial^2 f}{\partial z^2} + \frac{\partial}{\partial r} r^{-1} \frac{\partial}{\partial r}(rf) &= \left[\frac{2}{\Lambda} f - \frac{\varphi_0}{\Lambda\pi r}\right]\delta(z) \\ &= (4\pi/c) j_s(r,z),\end{aligned} \qquad (13)$$

where $\Lambda \equiv 2\lambda^2/d$ plays the role of an effective penetration depth. This equation was solved with a Hankel transform by Pearl,[6] who found

$$f(r,z) = \frac{\varphi_0}{2\pi}\int_0^\infty d\gamma \frac{J_1(\gamma r)}{1+\Lambda\gamma}\exp(-\gamma z) \qquad z>0, \qquad (14)$$

where J_1 is the Bessel function.[20] The corresponding

[20] See, for example, *Handbook of Mathematical Functions with Formulas, Graphs and Mathematical Tables*, edited by M. Abramowitz and I. A. Stegun (U.S. Government Printing Office, Washington, 1964), Natl. Bur. Std. Appl. Math. Ser. 55.

supercurrent is given by

$$\mathbf{j}_s(r,z)=\delta(z)\hat{\theta}\frac{\varphi_0 c}{8\pi\Lambda^2}\left[\mathbf{H}_1\left(\frac{r}{\Lambda}\right)-Y_1\left(\frac{r}{\Lambda}\right)-2\pi^{-1}\right], \qquad (15)$$

where $\mathbf{H}_1$ is the Struve function and Y_1 the Neumann function of order unity.[20] The limiting behavior is given by

$$\mathbf{j}_s(r)\approx\hat{\theta}\delta(z)(\varphi_0 c/4\pi^2)(1/\Lambda r) \qquad \text{for } r\ll\Lambda, \quad (16)$$

$$\mathbf{j}_s(r)\sim\hat{\theta}\delta(z)(\varphi_0 c/4\pi^2)(1/r^2) \qquad \text{for } r\gg\Lambda. \quad (17)$$

This behavior is to be contrasted with the current due to a vortex in a bulk sample, which has the form

$$\mathbf{j}_s(r)d=(\hat{\theta}\varphi_0 cd/8\pi^2\lambda^3)K_1(r/\lambda), \qquad (18)$$

for a vortex of length d. The limiting behavior of Eq. (18) is given by

$$\mathbf{j}_s(r)d\approx\hat{\theta}\frac{\varphi_0 c}{4\pi^2}\frac{d}{2\lambda^2 r} \qquad \text{for } r\ll\lambda,$$

$$\mathbf{j}_s(r)d\sim\hat{\theta}\frac{\varphi_0 c}{8\pi^2}\frac{d}{\lambda^3}\left(\frac{\pi\lambda}{2r}\right)^{1/2}\exp(-r/\lambda) \qquad \text{for } r\gg\lambda. \quad (19)$$

The microscopic magnetic field $\mathbf{h}$ in the film is just the curl of the vector potential Eq. (14), but for $z=0$ the γ integral is only conditionally convergent so that the Bessel function may not be differentiated under the integral sign. Instead, it is convenient to use the London equation

$$\mathbf{h}+(4\pi\lambda^2/c)\,\mathrm{curl}\,\mathbf{j}_s=\varphi_0\delta(\mathbf{r})\hat{z}, \qquad (20)$$

which is valid inside the superconductor in our narrow-core approximation. We thus obtain from Eq. (15)

$$h_z(r)\sim(\varphi_0/2\pi)(\Lambda/r^3) \qquad \text{for } r\gg\Lambda. \qquad (21)$$

Equation (21) shows that the magnetic field falls off sufficiently rapidly that the total magnetic flux associated with a single vortex remains finite and quantized, as can be seen by integrating the London equation (20). The *magnetic moment*, however, is defined by the integral

$$\mathbf{M}=\tfrac{1}{2}d\int\mathbf{r}\times\mathbf{j}_s d^2r. \qquad (22)$$

In a thin film, $\mathbf{M}$ depends linearly on the diameter of the plate R (assuming it to be circular for simplicity), while in a bulk sample the integral in Eq. (22) is cut off at λ. Similarly, the interaction energy between two vortices is obtained[6] by integrating the current $\mathbf{j}_s$,

$$V_{12}(r)=(\varphi_0^2/8\pi\Lambda)[\mathbf{H}_0(r/\Lambda)-Y_0(r/\Lambda)], \qquad (23)$$

which falls off as r^{-1} at large distances. These long-range magnetic interactions are just the microscopic expression of the demagnetizing effects considered in Sec. II. From the properties of single vortices, the macroscopic behavior can be derived directly[4,6,7] by a calculation analogous to Abrikosov's.[3] Since each vortex carries one quantum of flux, the induction $\mathbf{B}$, which is just the average of the microscopic field $\mathbf{h}(\mathbf{r})$, is given by $B=n\varphi_0$, where n is the vortex density.[21]

The field H_{c1}, which is determined from the self-energy of a vortex, depends on the current near the core; in the present approximation of vanishing core radius, H_{c1} is unchanged from its value in a bulk sample. In contrast, the *external* critical field H_{c1}^0 is determined from the interaction of H_0 with the magnetic moment of a vortex,[4,6,7] which is proportional to the radius R [cf. Eq. (22)], and we may thus rederive Eq. (4). The magnetization just above H_{c1}^0 depends on the interaction energy between vortices given in Eq. (23). Pearl (Ref. 6, p. 95) has shown that the relevant expression is the integral of Eq. (23) over all space, which is proportional to R. This behavior implies a finite slope $4\pi dM/dH_0$ for H_0 just above H_{c1}^0. However, the proof that the slope is exactly unity [as shown in Eq. (8)], and not some number of order R/d, which would still be essentially infinite, was not given by Pearl,[4,6] and appears to be more difficult to obtain from the microscopic point of view.

The value of $4\pi dM/dH$ at H_{c2} was calculated by Maki,[7] as a function of film thickness. This dependence is really a modification of the constitutive equation which will be discussed in Sec. IV. On the other hand, the slope $4\pi dM/dH_0$ depends on R/d even at H_{c2}, as mentioned in Sec. II; it is always less than $1+O(d/R)$, in contrast to $4\pi dM/dH$ which can become arbitrarily large.[22] The disagreement between theoretical predictions and the experimentally observed magnetization curves[16] is even more pronounced than was believed by Maki.[7] This discrepancy may be understood[2] by remarking that present experiments on films measure an extremely irreversible curve, which bears no relation to the reversible curves discussed here. The area under the reversible curves must be $H_c^2/8\pi$ (as shown in Sec. II), whereas the experimental areas are many orders of magnitude larger.

As pointed out by Pearl,[6,23] the effects described above in the case of thin films also occur at any surface of a bulk ($d\gg\lambda$) type-II superconductor which is perpendicular to the applied field. In a surface layer of thickness λ, the vortices behave as in a film, and interact over long distances. Such a modified interaction leads to a finite value for $4\pi dM/dH_0$, whenever there is a substantial fraction of surface perpendicular to $\mathbf{H}_0$. This long-range electromagnetic effect is just that calculated macroscopically in Sec. II; the value of $4\pi dM/dH_0$ is $1+O(d/R)$ when $d<R$, not $1+O(R/d)$, as stated by Pearl.[23]

[21] This expression for B differs from Maki's (Ref. 7) by a factor $2R/d$ because of an apparent confusion on his part between H and H_0.

[22] This distinction was not made in Sec. II of Maki's paper (Ref. 7).

[23] J. Pearl, J. Appl. Phys. **37**, 4139 (1966).

IV. DEPENDENCE OF CRITICAL FIELDS ON THICKNESS

In this section, we discuss the effect of varying film thickness[24] on the critical fields, or more precisely, on the constitutive relation. The basic parameter here is not d/R as in Sec. II, or d/λ as in Sec. III, but d/ξ.

Consider first the case $\kappa>1/\sqrt{2}$. The upper critical field $H_{c2}=\kappa\sqrt{2}H_c$ is then larger than H_c and the film is in the Abrikosov state for fields less than H_{c2} for any value of the ratio d/ξ. When $\kappa<1/\sqrt{2}$, on the other hand, H_{c2} is less than H_c and the magnetic properties depend critically on the parameter d/ξ. When the thickness is much larger than ξ, the film is in the intermediate state with a critical field H_c. This state is characterized by a first-order transition with superconducting domains whose size at the critical field is of order d or greater. As the thickness decreases, this domain size also decreases, but when d becomes less than ξ, the domains cannot shrink any further and the critical field[25] H_D becomes less than H_c. In the limit $d/\xi\ll1$, we have[25,26] $H_D^2\approx H_c^2d/\xi$. This value of the critical field H_D may be understood by noting that the field at the edge of a domain of height d and diameter ξ is roughly H_c, when the external field is H_D. At some point the field H_D becomes less than $H_{c2}=\sqrt{2}\kappa H_c$; this latter field then ceases to be a supercooling field and becomes the true critical field of the material. Thus, when $H_D<H_{c2}$ the transition is of second order and the state below H_{c2} is the mixed (Tinkham[1]) state we have been studying. It is interesting to note that in the somewhat unrealistic case that $\kappa\ll1$ and $d\ll\xi$, superconductivity would be completely destroyed at a field H_{c2} which is much less than H_c. The magnetic energy of this field $H_{c2}^2/8\pi$ is much less than the condensation energy $H_c^2/8\pi$, but there is no mechanism for superconductivity in fields larger than H_{c2}, since the superconducting domains would have to be smaller than ξ. The critical thickness is found by equating H_D and H_{c2}, which yields $d_c\approx\xi\kappa^2$ in the limit $d\ll\xi$. This has been calculated more accurately for arbitrary ratio d/ξ by Guyon, Caroli and Martinet,[26] by Maki,[7] and by Lasher.[13] The last two authors computed the limit of stability of the mixed state by finding the thickness d_c for which the slope of the magnetization curve dM/dH at H_{c2} vanished.

We turn now to the question of the core structure. Unless the value of κ is very large, the core size will not be small and the narrow core approximation made above will not be valid. The core structure is difficult to calculate even in bulk materials, so that only rough qualitative estimates can be made in films. According to Pearl's calculations[6] the field H_{c1} is given by $H_{c1}\approx\kappa^{-1}H_c(\lambda^2/d\xi)^{2/3}$ and the core radius is approximately $r_c\approx(24\lambda^2/d)^{1/3}\xi^{2/3}$. The core radius only increases as $d^{-1/3}$ with decreasing d, whereas the effective penetration depth $\Lambda=2\lambda^2/d$ varies as d^{-1}. This difference means that very thin films have a large "effective κ," defined by $\kappa_{\mathrm{eff}}=\Lambda/r_c$. It is also interesting to note that all quantities have stronger temperature dependences than in bulk materials. The "effective κ" [$\kappa_{\mathrm{eff}}\approx(\lambda^2/d\xi)^{2/3}$] diverges at the critical temperature, as does the slope of the magnetization $4\pi dM/dH$.[27]

V. LATTICE STABILITY IN THIN FILMS

We shall now consider the stability of vortex lattices in thin films. The calculations described below are valid for $H_{c1}\lesssim H\ll H_{c2}$, where the hydrodynamic model[14] is applicable. Near H_{c2}, a different approximation is necessary; for completeness, the behavior in the region of H_{c2} is briefly discussed at the end of this section. In the limit of very thin films ($d\ll\lambda$), the formulas of I, Sec. III must be evaluated for the current (15), which corresponds to the interaction function [compare Eq. (I.21)]

$$f(r)=\tfrac{1}{2}\pi(r\Lambda)^{-1}[\mathbf{H}_1(r/\Lambda)-Y_1(r/\Lambda)-2\pi^{-1}]. \quad (24)$$

Here $\mathbf{H}_1(x)$ is again a Struve function.[28] The vibration frequencies are given by Eqs. (I.26)–(I.28):

$$\omega^2=\eta^2-\alpha^2-\xi^2, \quad (25)$$

where

$$\alpha=(4\pi)^{-1}\bar{\kappa}\sum_j{}'[1-\exp(i\mathbf{q}\cdot\mathbf{R}_j)][-2X_jY_j/R_j]f'(R_j), \quad (26)$$

$$\xi=(4\pi)^{-1}\bar{\kappa}\sum_j{}'(1-\exp(i\mathbf{q}\cdot\mathbf{R}_j))(X_j^2-Y_j^2)R_j^{-1}f'(R_j), \quad (27)$$

$$\eta=-(4\pi)^{-1}\bar{\kappa}\sum_j{}'(1-\exp(i\mathbf{q}\cdot\mathbf{R}_j))\times\{r^{-1}(d/dr)[r^2f(r)]\}\big|_{r=R_j}. \quad (28)$$

Here the sums run over the lattice points $\{\mathbf{R}_j\}$ excluding the origin, and $\bar{\kappa}=h/2m$.

The exact evaluation of these lattice sums is very difficult and is given in detail in Appendix B. For a preliminary treatment, we shall instead consider the continuum model, which was shown in I to make qualitatively correct predictions. In the continuum approximation, the sums in Eqs. (26)–(28) are re-

[24] Clearly when d varies, the mean free path l also varies, and this causes changes in λ, ξ and κ. We are not concerned here with this dependence; we shall merely assume that for any film, the lengths λ and ξ have given values, which may be larger or smaller than the thickness d. The parameter κ is defined to be λ/ξ, and we consider it to be a free parameter, independent of d, although for a *given* material, κ will depend on d through the mean free path.

[25] E. A. Davies, Proc. Roy. Soc. (London) **A255**, 407 (1960).

[26] E. Guyon, C. Caroli, and A. Martinet, J. Phys. **25**, 683 (1964).

[27] This was noted by Maki (Ref. 7). However, the quantity $4\pi\, dM/dH_0$ is still less than 1, as we point out in Sec. II.

[28] G. N. Watson, *A Treatise on the Theory of Bessel Functions* (Cambridge University Press, Cambridge, England, 1962), pp. 329, 436.

placed by integrals

$$\eta=-\frac{n\bar{\kappa}}{4\pi}\int_b^\infty r\,dr\int_0^{2\pi}d\theta \times[1-\exp(i\mathbf{q}\cdot\mathbf{r})]r^{-1}\frac{d}{dr}[r^2f(r)], \quad (29)$$

$$\xi-i\alpha=\frac{n\bar{\kappa}}{4\pi}\int_b^\infty r\,dr\int_0^{2\pi}d\theta \times[1-\exp(i\mathbf{q}\cdot\mathbf{r})]rf'(r)\exp(2i\theta), \quad (30)$$

where $n=B/\varphi_0$ is the vortex density. The integrals extend over the whole lattice, excluding the area associated with the single vortex at the origin, which fixes the lower cutoff as $b=(n\pi)^{-1/2}$. In Appendix A, it is shown that

$$\eta=\tfrac{1}{2}n\bar{\kappa}\{b^2f(b)[1-J_0(qb)]+q\Lambda I\}, \quad (31)$$

$$|\xi-i\alpha|=\tfrac{1}{2}n\bar{\kappa}\{b^2f(b)J_2(qb)+q\Lambda I\}; \quad (32)$$

I is a definite integral discussed below. These equations are valid for any vortex lattice with an arbitrary current distribution f. The problem is thus reduced to the evaluation of a single integral

$$\begin{aligned} I&\equiv\Lambda^{-1}\int_b^\infty r^2\,drJ_1(qr)f(r)\\ &=(1+q\Lambda)^{-1}-\Lambda^{-1}\int_0^b r^2\,drJ_1(qr)f(r)\\ &=1+O(q\Lambda)+O(qb), \qquad (q\Lambda\ll1,\ qb\ll1) \end{aligned} \quad (33)$$

where the explicit form of the function f [Eq. (24)] has now been used. In the long-wavelength limit ($qb\ll1$), Eq. (25) then yields

$$\omega^2=(\tfrac{1}{4}n\bar{\kappa})^2q^3b^3(1+q\Lambda)^{-1}\tfrac{1}{2}\pi[\mathbf{H}_1(b/\Lambda)-Y_1(b/\Lambda)-2\pi^{-1}]. \quad (34)$$

Two limiting cases are especially simple: In a low-density lattice ($H_{c1}\lesssim H$), the vibration frequency is given by

$$\omega=\tfrac{1}{4}(eB/mc)q^{3/2}\Lambda(n\pi)^{-1/4}, \qquad (b\gg\Lambda) \quad (35)$$

while in an intermediate-density lattice ($H_{c1}\ll H\ll H_{c2}$), the vibration frequency is

$$\omega=\tfrac{1}{4}(eB/mc)q^{3/2}\Lambda^{1/2}(n\pi)^{-1/2}, \qquad (qb\ll q\Lambda\ll1) \quad (36a)$$

$$\omega=\tfrac{1}{4}(eB/mc)q(n\pi)^{-1/2}, \qquad (qb\ll1\ll q\Lambda). \quad (36b)$$

These results are only valid if $qR\gg1$, because otherwise the assumption of translational invariance fails. For larger values of q than those considered in Eqs. (35) and (36), one can expand Eqs. (25) and (31)–(33) to find ω^2 as an analytic power series in qb, since the Bessel functions in Eqs. (31)–(33) are analytic functions with no singularities in the finite complex plane.

Instead of Eq. (24), it is also interesting to consider an approximate form of the supercurrent

$$f(r)=\Lambda r^{-2}(r+\Lambda)^{-1}, \quad (37)$$

suggested by Pearl.[6] In this case, the calculated vibration frequency agrees with Eqs. (35) and (36a) in lowest order, but the corrections are of order $q\Lambda\ln(q\Lambda)$ if $b\ll\Lambda$; a comparison with the exact result [Eqs. (31)–(33)] shows the logarithmic corrections to be spurious.

The continuum approximation predicts real vibration frequencies in the long-wavelength limit, which suggests that a periodic array of vortices in a thin film represents a stable configuration. Naturally, this model is unable to predict the precise form of the equilibrium lattice, which requires an evaluation of the lattice sums (26)–(28). For simplicity, we have considered only a triangular lattice, which is the stable structure in a bulk type-II superconductor for all applied fields.[14] The calculations are very long and are described in Appendix B. In the long-wavelength limit ($qa\ll1$, $q\Lambda\ll1$, but $qR\gg1$) the vibration frequency is

$$\omega=\tfrac{1}{4}(eB/mc)q^{3/2}\Lambda(n\pi)^{-1/4}C^{1/2}, \qquad (a\gg\Lambda)$$

$$\omega=\tfrac{1}{4}(eB/mc)q^{3/2}\Lambda^{1/2}(n\pi)^{-1/2}, \qquad (a\ll\Lambda) \quad (38)$$

where $C\approx1.10611$. Here a is the lattice spacing and $n=2/\sqrt{3}a^2$. These expressions agree almost exactly with Eqs. (35) and (36a) derived in the continuum approximation; they show that a triangular lattice structure is stable for both limiting densities $a\gg\Lambda$ and $a\ll\Lambda$, assuming only that $r_c\ll a$, so that the vortex cores are well separated. Unfortunately, the methods of Appendix B cannot treat the limit $qa\ll1\ll q\Lambda$ for the triangular lattice, but the behavior is probably similar to the continuum model [Eq. (36b)].[29]

In principle, it is also possible to evaluate the lattice sums for a square array; the resulting vibration frequencies would then depend on the angle between the propagation vector $\mathbf{q}$ and the symmetry direction of the lattice [compare the corresponding expression for a bulk sample in Eq. (I. 36)]. These calculations have not been attempted, since they would be considerably more difficult than those in Appendix B. Nevertheless, we conjecture that the square lattice is unstable with respect to waves propagating in certain directions, in analogy with the situation in bulk samples.

[29] It is also interesting to compare these results with the (similar) situation in bulk type-II superconductors (Ref. 14). The cutoff parameter d [Eq. (I.A2)] introduced in the continuum approximation must be taken as $(n\pi)^{-1/2}$; the corresponding vibration frequencies both for the continuum model [Eq. (I.31)] and for the triangular lattice [Eq. (I.38)] then reduce to $\omega=\frac{1}{4}(eB/cm)q^2\lambda(n\pi)^{-1/2}$ for $qn^{-1/2}\ll q\lambda\ll1$. In the other limit $qn^{-1/2}\ll1\ll q\lambda$, Eq. (I.31) reduces to $\omega=\frac{1}{4}(eB/mc)q(n\pi)^{-1/2}$, which is identical with Eq. (36b). As in the thin film, this last limiting case cannot be evaluated except in the continuum approximation.

The above stability calculations assume that the vortex cores are far apart ($H \ll H_{c2}$) and apply to a material with arbitrary κ in the limit of a thin film (in fact we need $\kappa d/\xi \ll 1$). As we increase the thickness, however, the behavior of the system depends on the value of κ. If $\kappa > 1/\sqrt{2}$, then the interaction (24) presumably merges continuously with the bulk interaction, which was shown in I to predict a stable triangular lattice. In contrast, when $\kappa < 1/\sqrt{2}$, the "effective κ" decreases as the thickness increases, and the region in which the vortices are well separated ($H_{c1} \ll H \ll H_{c2}$) shrinks to zero. Exact calculations are then possible only near the upper critical field, where the stability may be tested for arbitrary κ by evaluating the free energy to lowest order in $|\Psi|^2$. This computation has been performed numerically by Kleiner, Roth, and Autler[12] for bulk materials, and by Lasher[13] for films. In bulk samples, the triangular lattice has the lowest Gibbs free energy near H_{c2} for all $\kappa > 1/\sqrt{2}$. In a film for which $d \ll \xi$, the triangular lattice also has the lowest Gibbs free energy near H_{c2} for all κ. We expect, although it has not been proved, that the triangular array represents the equilibrium state of a type-II superconductor ($\kappa > 1/\sqrt{2}$) for all values of the thickness. On the other hand, if $\kappa < 1/\sqrt{2}$, then the bulk sample must be in the intermediate state.[25] Lasher[13] showed that as the thickness increases, the transition from the triangular array in the mixed state ($d \ll \xi$) to the intermediate state[25] occurs through a complicated sequence of hexagonal lattices, each flux line containing more than one quantum.

In a bulk sample near H_{c2}, it has also been proved *analytically* that the triangular lattice has the lowest Gibbs free energy.[30] It is first shown that each vortex carries one quantum of flux, and the proof then depends only on the properties of the theta functions. Since the form of the free energy for a thin film ($d \ll \xi$) near H_{c2} is identical with that in bulk material,[7,13] the proof remains valid and confirms Lasher's detailed calculations that the triangular lattice is the stable state in very thin films. As the thickness increases, the quantum number of flux carried by each vortex also increases, and a similar (but more complicated) analytic proof could presumably reproduce Lasher's other conclusions.

VI. CRITIQUE OF LATTICE DYNAMICS

In the previous section, the stability of a vortex lattice was treated in purely hydrodynamic terms. The basic assumption of this approach is that the motion of a given vortex arises solely from the induced velocity at the position of its core due to all the other vortices in the system. If the vortices are placed at the positions $\{\mathbf{r}_j\}$, then the translational velocity $\dot{\mathbf{r}}_i$ of the ith vortex is given by[14]

$$\dot{\mathbf{r}}_i = \mathbf{v}(\mathbf{r}_i) = \sum_j{}' \mathbf{v}_0(\mathbf{r}_i - \mathbf{r}_j), \tag{39}$$

where $\mathbf{v}_0(\mathbf{r})$ is the velocity field of a vortex at the origin

$$\mathbf{v}_0(\mathbf{r}) = (2\pi)^{-1}\bar{\kappa}\hat{z} \times \mathbf{r} f(r). \tag{40}$$

The hydrodynamic point of view differs from the usual theory of lattice dynamics, where the interaction energy V is considered the fundamental quantity. It is therefore interesting to recast Eq. (40) in the conventional dynamical form. Let $V_{12} = V(r_{12})$ be the interaction energy per unit length between two vortices situated at $\mathbf{r}_1$ and $\mathbf{r}_2$. The total interaction energy per unit length of lattice is

$$V = \tfrac{1}{2} \sum_{jk}{}' V_{jk}, \tag{41}$$

where the primed sum is over j and k separately, omitting the terms $j = k$. The force $\mathbf{F}_i$ acting on the ith vortex is

$$\mathbf{F}_i = -\nabla_i V = -\sum_j{}' (\mathbf{r}_i - \mathbf{r}_j) r_{ij}^{-1} V_{ij}', \tag{42}$$

where V_{ij}' means $V'(r_{ij})$. Since the interaction energy V_{12} can be interpreted as the work done in bringing the two vortices together from infinity,[6,31] it can be shown that

$$V'(r) = -(2\pi)^{-1}\rho\bar{\kappa}^2 r f(r), \tag{43}$$

where f is defined in Eq. (40), and $\rho \equiv nm$ is the mass density of superelectrons. Thus the fluid velocity at the position of the ith vortex may be rewritten as

$$\mathbf{v}(\mathbf{r}_i) = (\rho\bar{\kappa})^{-1}\hat{z} \times \mathbf{F}_i, \tag{44}$$

which proves an assertion made in I, Sec. V. This represents a general result valid for all vortex systems, independent of the details of the velocity pattern $f(r)$. A combination of Eqs. (44) and (39) yields the basic equation of vortex dynamics

$$\mathbf{F}_i = -\rho\bar{\kappa}\hat{z} \times \dot{\mathbf{r}}_i, \tag{45}$$

which shows that a vortex moves perpendicular to an applied force.

Equation (45) is fundamentally different from the usual equations of motion in crystal lattices, which obey Newtonian dynamics. In order to emphasize this distinction, we shall consider a hypothetical system of parallel rods interacting through the same potential V_{12}. The corresponding Newtonian equations of motion are

$$M\ddot{\mathbf{r}}_i = \mathbf{F}_i = -\nabla_i V, \tag{46}$$

where M is the mass per unit length of rod. In equilibrium, the system is assumed to form a regular lattice

[30] G. Eilenberger, Z. Physik **180**, 32 (1964); D. St. James, G. Sarma, and E. J. Thomas, *Type-II Superconductivity* (Pergamon Press, Ltd., London, 1967).

[31] See Ref. 8, pp. 64–6.

specified by the set of points $\{\mathbf{R}_j\}$. If the rods are displaced to new positions $\mathbf{R}_i+\mathbf{u}_i$, the corresponding Newtonian equations are

$$Md^2\mathbf{u}_i/dt^2 = \sum_j{}' \{(\mathbf{u}_i-\mathbf{u}_j)f_{ij}+\mathbf{R}_{ij}[\mathbf{R}_{ij}\cdot(\mathbf{u}_i-\mathbf{u}_j)]R_{ij}^{-1}f_{ij}'\}, \tag{47}$$

where Eq. (43) has been used to replace V' by f. For a large lattice ($qR\gg1$), plane waves may be used to decouple these equations of motion, so that we may assume a solution of the form

$$\mathbf{u}_j=\mathbf{s}\exp(i\mathbf{q}\cdot\mathbf{R}_j-i\omega t). \tag{48}$$

This equation leads to an eigenvalue condition of the form

$$(M\omega^2/\rho\bar{\kappa})s_x=(\eta-\xi)s_x+\alpha s_y,$$
$$(M\omega^2/\rho\bar{\kappa})s_y=\alpha s_x+(\eta+\xi)s_y, \tag{49}$$

where α, η, and ξ are defined in Eqs. (26)–(28). The frequencies of small oscillations in the hypothetical Newtonian dynamical system are easily found to be

$$\omega^2=(\rho\bar{\kappa}/M)[\eta\pm(\alpha^2+\xi^2)^{1/2}], \tag{50}$$

which should be compared with Eq. (25), based on vortex dynamics.

It is interesting that the same combination of lattice sums appears in both dynamical models. If the interaction potential V_{ij} is such that the system is stable with Newtonian dynamics, it immediately follows that the system is also stable with vortex dynamics. The converse is clearly untrue. Stability in vortex dynamics is independent of the sign of the interaction potential, since only the squares of the lattice sums appear in Eq. (25). In contrast, η changes sign with V_{ij}, so that a stable system in Newtonian dynamics is rendered unstable merely by changing the sign of the potential. This demonstrates that vortex systems are inherently more stable than Newtonian systems, and intuitive ideas based on the behavior of crystalline solids may not be applicable to vortex lattices.[11]

The above discussion is valid for all wavelengths $\mathbf{q}$, subject only to the restriction that $qR\gg1$. Thus these considerations are more general than elasticity theory, which assumes that the wavelength is long compared with the interparticle spacing ($qa\ll1$). If the interaction potential V_{ij} has a sufficiently short range, then it is permissible to expand the exponentials appearing in Eqs. (26)–(28) under the summation signs; in this case, the coefficients α, ξ, and η are obviously of order q^2 for a lattice with inversion symmetry. It is then easy to estimate the form of the dispersion relation for lattice vibrations from Eqs. (25) and (50)

$$\omega\propto q^2 \quad \text{(vortex dynamics)}, \tag{51}$$

$$\omega\propto q \quad \text{(Newtonian dynamics)}, \tag{52}$$

which agrees with the vibrations of an elastic continuum.[32,33] The fundamental difference between Eq. (51) and Eq. (52) arises from the appearance of velocities in the equations of vortex dynamics Eq. (45), instead of accelerations as in the conventional Newtonian equations Eq. (46).

For many systems of physical interest the potential V_{ij} is long range, and direct expansion of Eqs. (26)–(28) in powers of $\mathbf{q}$ is impossible. This means that the dispersion relation will not take the form (51) or (52) at long wavelengths, and it also indicates a failure of elasticity theory. In particular, the interaction between two flux lines in a thin film has been shown to give a dispersion relation of the form $\omega\propto q^{3/2}$. Thus there can be no elastic theory in this case and related concepts, such as the shear modulus, are therefore inapplicable.[11]

It is generally true that a long-range potential implies a decreased exponent of q in the dispersion relation. A well-known example of this behavior is the collective mode in an interacting Fermi gas, which appears as a compressional wave in a neutral system ($\omega\propto q$) and as a plasma mode in a charged system ($\omega=\omega_p$).[34] It must be emphasized, however, that a long-range potential in no way precludes a regular lattice, which occurs, for example, in a low-density electron gas.[35] The infinite Coulomb energy of this system is cancelled by a uniform positive background to ensure charge neutrality. The main residual effect of the long-range Coulomb repulsion is that the difference in free energy between various lattices is extremely small. In a thin superconducting film, on the other hand, the free energy per vortex actually diverges as the sample becomes infinite, since there is nothing corresponding to the uniform positive background. Thus the free energy associated with a given lattice structure cannot be calculated directly. In principle, it would be possible to compare different regular arrays in a large but finite system and then to let the sample become infinite; such an approach is very difficult and has not been attempted by us. In contrast, the lattice sums appearing in the vibration frequency involve an extra derivative of V_{ij} and converge in this case even for an infinite lattice. Hence the stability of a triangular lattice for $H\ll H_{c2}$ is independent of the size of the sample. Near H_{c2}, where the vortex cores overlap, the free energy per vortex is independent of sample size, and all stability calculations have been based on comparison of the free energy for different arrangements[12,13] of flux lines; no dynami-

[32] P. G. de Gennes and J. Matricon, Rev. Mod. Phys. **36**, 45 (1964); J. Matricon, Phys. Letter **9**, 289 (1964).

[33] See, for example, M. Born and K. Huang, *Dynamical Theory of Crystal Lattices* (Oxford University Press, London, 1964).

[34] See, for example, P. Nozières and D. Pines, *Quantum Liquids* (W. A. Benjamin, Inc., New York, 1966), Vol. I.

[35] E. P. Wigner, Trans. Faraday Soc. **34**, 678 (1938); C. H. Herring, in *Magnetism*, edited by G. T. Rado and H. Suhl (Academic Press Inc., New York, 1966), Vol. IV, Sec. IV.

cal theory of lattice vibrations appears possible in this domain.

VII. CONCLUSION

We therefore consider it well established that an ideal superconducting thin film would exhibit a triangular lattice structure. In real films, the main factors which would destroy lattice order are nonuniformity of thickness and edge effects, both of which lead to irreversibility. A quantitative estimate of these effects is difficult.

It may be possible to observe the lattice from outside the sample because of its inhomogeneous magnetic field.[36] Unfortunately this inhomogeneity is only observable over a distance of the order of the lattice spacing a from the surface. Indeed, if the field $\mathbf{H}$ is assumed to be periodic in x and y it may be expanded in a Fourier series

$$\mathbf{H}(\mathbf{r},z)=\sum_l \mathbf{a}_l(z)\exp(i\mathbf{k}_l\cdot\mathbf{r}),\qquad (z>0)\quad (53)$$

where $\mathbf{k}_l$ are the reciprocal lattice vectors of the vortex lattice, and $\mathbf{r}$ is a vector in the x-y plane. Since the magnetic field in free space is both irrotational and solenoidal, it follows that $\mathbf{H}$ must be of the form

$$\mathbf{H}(\mathbf{r},z)=\sum_l C_l(\hat{z}-i\hat{k}_l)\exp(i\mathbf{k}_l\cdot\mathbf{r})\exp(-k_lz),\qquad (z>0),\quad (54)$$

where C_l are constants determined from the boundary condition at $z=0$. At large z, only the contribution from the smallest $\mathbf{k}_l$ remains, and for a triangular lattice we find

$$\mathbf{H}(\mathbf{r},z)\sim C_0\hat{z}+\boldsymbol{\varphi}(x,y)\exp[-(4\pi z/a\sqrt{3})]+O(\exp[-(4\pi\sqrt{3}z/a)]).\quad (55)$$

Here $\boldsymbol{\varphi}(x,y)$ is a periodic vector function given by

$$\boldsymbol{\varphi}(x,y)=\sum_l C_l(\hat{z}-i\hat{k}_l)\exp(i\mathbf{k}_l\cdot\mathbf{r}),\quad (56)$$

where the sum is over the six smallest reciprocal lattice vectors. Thus the periodicity of the magnetic field in free space vanishes exponentially with a characteristic length $\sqrt{3}a/4\pi$.[37] This description applies both to a thin film and to the surface of bulk material.

ACKNOWLEDGMENTS

We are grateful for useful discussions with M. Tinkham and P. W. Anderson.

APPENDIX A

In this Appendix, the sums required for the vibration frequencies are evaluated in the continuum approximation. The necessary integrals are

$$\xi-i\alpha=(4\pi)^{-1}n\bar{\kappa}\int_b^\infty r^2\,drf'(r)\int_0^{2\pi}d\theta\exp(2i\theta)\times[1-\exp(i\mathbf{q}\cdot\mathbf{r})],$$

$$\eta=-(4\pi)^{-1}n\bar{\kappa}\int_b^\infty dr[r^2f(r)]'\int_0^{2\pi}d\theta\times[1-\exp(i\mathbf{q}\cdot\mathbf{r})],\quad (A1)$$

where the primes denote differentiation with respect to r. The integrals over angle yield

$$\xi-i\alpha=\tfrac{1}{2}n\bar{\kappa}\exp(2i\chi)\int_b^\infty r^2\,drJ_2(qr)f'(r),$$

$$\eta=-\tfrac{1}{2}n\bar{\kappa}\int_b^\infty dr[1-J_0(qr)][r^2f(r)]',\quad (A2)$$

where the propagation vector $\mathbf{q}$ has been resolved in polar coordinates (q,χ). Each of these expressions may be integrated by parts, and Eq. (A2) therefore reduces to

$$\xi-i\alpha=-\tfrac{1}{2}n\bar{\kappa}\exp(2i\chi)[b^2f(b)J_2(qb)+q\Lambda I],$$
$$\eta=\tfrac{1}{2}n\bar{\kappa}\{b^2f(b)[1-J_0(qb)]+q\Lambda I\}.\quad (A3)$$

Hence it is necessary only to evaluate a single definite integral

$$I=\Lambda^{-1}\int_b^\infty r^2\,drf(r)J_1(qr).\quad (A4)$$

It is easy to verify that this formulation reproduces the results of I, Appendix A, if f is chosen as $(\lambda r)^{-1}K_1(r/\lambda)$, which is appropriate to a bulk superconductor. Here, we shall consider the interaction function

$$f(r)=\tfrac{1}{2}\pi(\Lambda r)^{-1}[\mathbf{H}_1(r/\Lambda)-Y_1(r/\Lambda)-2\pi^{-1}],\quad (A5)$$

which provides an exact description of a vortex in a thin film. This function has the following limiting behavior:

$$f(r)\approx r^{-2}\qquad (r\ll\Lambda),$$
$$f(r)\sim\Lambda r^{-3}\qquad (r\gg\Lambda).\quad (A6)$$

The long-range behavior shows that the integral I cannot be expanded in ascending powers of q. It is, however, possible to rewrite I as

$$I=I_1+I_2,\quad (A7)$$

where

$$I_1=\Lambda^{-1}\int_0^\infty r^2\,drf(r)J_1(qr),\quad (A8a)$$

$$I_2=-\Lambda^{-1}\int_0^b r^2\,drf(r)J_1(qr);\quad (A8b)$$

the first term may be integrated exactly while the

[36] S. T. Wang, L. Challis, and W. A. Little, in Proceedings of the Tenth International Conference on Low Temperature Physics LT10, Moscow, 1966 (to be published).

[37] We are indebted to Professor M. Tinkham for a discussion of this point.

second term is finite and may be evaluated by expanding the Bessel function in powers of qr.

Equation (A8a) may be rewritten with the following integral representation[28]:

$$\mathbf{H}_1(\zeta)-Y_1(\zeta)-2\pi^{-1}=Y_{-1}(\zeta)-\mathbf{H}_{-1}(\zeta)$$
$$=2\pi^{-1}\int_0^\infty dx x(x+1)^{-1}J_1(\zeta x), \tag{A9}$$

which yields

$$I_1=\Lambda^{-2}\int_0^\infty dx x(x+1)^{-1}\int_0^\infty r dr J_1(qr)J_1(xr/\Lambda). \tag{A10}$$

This integral is a repeated Hankel transform, and we therefore find

$$I_1=(1+q\Lambda)^{-1}=1-q\Lambda(1+q\Lambda)^{-1}$$
$$=1+O(q\Lambda) \qquad (q\Lambda\ll 1). \tag{A11}$$

The second integral I_2 may be computed to leading order in q by writing $J_1(qr)\approx\frac{1}{2}qr$

$$-I_2\approx\frac{\pi q}{4\Lambda^2}\int_0^b r^2\,dr\left[\mathbf{H}_1\left(\frac{r}{\Lambda}\right)-Y_1\left(\frac{r}{\Lambda}\right)-2\pi^{-1}\right]$$
$$=\tfrac{1}{4}\pi qb\{b\Lambda^{-1}[\mathbf{H}_2(b/\Lambda)-Y_2(b/\Lambda)]$$
$$-(4\Lambda/\pi b)-2(3\pi)^{-1}b^2\Lambda^{-2}\}. \tag{A12}$$

These expressions may be used to verify the vibration frequencies given in Sec. V for the continuum approximation.

It is also interesting to consider the approximate interaction function suggested by Pearl[6]

$$f(r)=\Lambda r^{-2}(r+\Lambda)^{-1}, \tag{A13}$$

which reproduces the exact expression Eq. (A5) both for $r\ll\Lambda$ and for $r\gg\Lambda$. The corresponding infinite integral is

$$I_1=\int_0^\infty dr J_1(qr)\,(r+\Lambda)^{-1}$$
$$=\Lambda^{-1}\int_0^\infty r dr J_1(qr)[r^{-1}-(r+\Lambda)^{-1}]. \tag{A14}$$

It is rather remarkable that this expression is just the integral used above in Eq. (A9), and we find

$$I_1=(q\Lambda)^{-1}+1-\tfrac{1}{2}\pi[\mathbf{H}_1(q\Lambda)-Y_1(q\Lambda)]. \tag{A15}$$

Inspection of the relevant series expansion shows that

$$I_1\approx 1-\tfrac{1}{2}q\Lambda[\ln(2/q\Lambda)-\gamma+\tfrac{1}{2}]+O(q^2\Lambda^2), \tag{A16}$$

where $\gamma=0.577\cdots$ is Euler's constant. The other integral I_2 is given approximately as

$$I_2\approx-\tfrac{1}{2}q\int_0^b r dr(r+\Lambda)^{-1}$$
$$=\tfrac{1}{2}\{q\Lambda\ln[1+(b/\Lambda)]-qb\}. \tag{A17}$$

Thus the approximate expression for the vortex velocity field Eq. (A13) produces spurious logarithmic corrections to the dispersion relation; such terms are clearly absent in the exact expressions obtained from Eqs. (A8b) and (A11).

APPENDIX B

The previous Appendix contains the evaluation of the vibration frequencies of a vortex lattice in a thin film using the continuum approximation; we shall here describe the corresponding exact results for the particular case of a triangular lattice. The vibrations are completely determined by three lattice sums

$$\eta=-(4\pi)^{-1}\bar{\kappa}\sum_j{}'[1-\exp(i\mathbf{q}\cdot\mathbf{R}_j)][2f(R_j)+R_jf'(R_j)],$$
$$\alpha=-(4\pi)^{-1}\bar{\kappa}\sum_j{}'[1-\exp(i\mathbf{q}\cdot\mathbf{R}_j)][2X_jY_jR_j^{-1}f'(R_j)],$$
$$\xi=(4\pi)^{-1}\bar{\kappa}\sum_j{}'[1-\exp(i\mathbf{q}\cdot\mathbf{R}_j)][(X_j^2-Y_j^2)R_j^{-1}f'(R_j)], \tag{B1}$$

where f is given in Eq. (A5). It is not possible to evaluate these quantities for arbitrary $\mathbf{q}$, however, and the present work will be restricted to the long-wavelength limit. The main difficulty is the long range of the interaction, since the sums diverge if the exponential is expanded in ascending powers of q. It is convenient to separate f into two parts

$$f(r)=f_0(r)+\bar{f}(r), \tag{B2}$$

where

$$f_0(r)=\Lambda r^{-3},$$
$$\bar{f}(r)=\tfrac{1}{2}\pi(\Lambda r)^{-1}[\mathbf{H}_1(r/\Lambda)-Y_1(r/\Lambda)]-(r\Lambda)^{-1}-\Lambda r^{-3}. \tag{B3}$$

Each lattice sum then separates into two terms denoted by $\{\eta_0,\alpha_0,\xi_0\}$ and $\{\bar{\eta},\bar{\alpha},\bar{\xi}\}$, in which f in Eq. (B1) is replaced by f_0 and $\bar{f}$, respectively. The sums involving f_0 may be evaluated exactly with the Ewald method[38]; furthermore, it is straightforward to verify that

$$\bar{f}(r)\sim O(\Lambda^3/r^5), \qquad (r\gg\Lambda) \tag{B4}$$

which allows an expansion of the barred lattice sums through terms of order q^2.

Long-Range Contributions

The long-range contributions are most easily evaluated by considering the following quantity:

$$\Sigma_n(\mathbf{q})=\sum_j{}'R_j^{-n}\exp(i\mathbf{q}\cdot\mathbf{R}_j). \tag{B5}$$

All the relevant lattice sums may be expressed in terms of Eq. (B5) as

$$\eta_0=(4\pi)^{-1}\bar{\kappa}\Lambda[\Sigma_3(0)-\Sigma_3(\mathbf{q})], \tag{B6}$$
$$-\xi_0+i\alpha_0=(4\pi)^{-1}3\bar{\kappa}\Lambda[\Sigma_{xy}(0)-\Sigma_{xy}(\mathbf{q})], \tag{B7}$$

[38] See, for example, J. M. Ziman, *Principles of the Theory of Solids* (Cambridge University Press, Cambridge, England, 1964), pp. 37–42.

where

$$\Sigma_{xy}(\mathbf{q})=\sum_j{}' \exp(i\mathbf{q}\cdot\mathbf{R}_j)(X_j+iY_j)^2R_j^{-5},$$

$$=-\left[\left(\frac{\partial}{\partial q_x}\right)^2-\left(\frac{\partial}{\partial q_y}\right)^2+2i\frac{\partial^2}{\partial q_x\partial q_y}\right]\Sigma_5(\mathbf{q}). \quad \text{(B8)}$$

Since $\sum_j{}'R_j^{-3}$ converges absolutely, Eqs. (B6) and (B7) are well defined.

Equation (B6) may be rewritten with the Ewald method using the identity

$$R_j^{-3}=4\pi^{-1/2}\int_0^\infty d\zeta\zeta^2\exp(-\zeta^2R_j^2). \quad \text{(B9)}$$

Substitution of Eq. (B9) into Eq. (B5) yields

$$\Sigma_3(\mathbf{q})=\Sigma_3^{(1)}(\mathbf{q})+\Sigma_3^{(2)}(\mathbf{q}), \quad \text{(B10)}$$

where

$$\Sigma_3^{(1)}(\mathbf{q})=4\pi^{-1/2}\sum_j{}'\exp(i\mathbf{q}\cdot\mathbf{R}_j)\int_0^Z d\zeta\zeta^2\exp(-\zeta^2R_j^2), \quad \text{(B11)}$$

$$\Sigma_3^{(2)}(\mathbf{q})=4\pi^{-1/2}\sum_j{}'\exp(i\mathbf{q}\cdot\mathbf{R}_j)\int_Z^\infty d\zeta\zeta^2\exp(-\zeta^2R_j^2). \quad \text{(B12)}$$

Here Z is an arbitrary constant that is eventually chosen to simplify the computations. The definite integral in Eq. (B12) becomes exponentially small as $R_j\to\infty$, so that it is now permissible to expand $\Sigma_3^{(2)}$ in powers of $\mathbf{q}$, which yields

$$\Sigma_3^{(2)}(\mathbf{q})=4\pi^{-1/2}\sum_j{}'[1+i\mathbf{q}\cdot\mathbf{R}_j-\tfrac{1}{2}(\mathbf{q}\cdot\mathbf{R}_j)^2+\cdots]\times\int_Z^\infty d\zeta\zeta^2\exp(-\zeta^2R_j^2). \quad \text{(B13)}$$

The linear term in Eq. (B13) vanishes by symmetry. The quadratic term is of the form

$$\sum_j{}' q^2R_j^2F(R_j)\cos^2(\theta_j-\chi),$$

which may be simplified by summing over concentric circles containing equivalent neighbors. For a triangular lattice, the angular factor is then replaced by its average value $\frac{1}{2}$ (see, for example, I, Appendix B). A straightforward calculation leads to the result

$$\Sigma_3^{(2)}(0)-\Sigma_3^{(2)}(\mathbf{q})=q^2Z(2\pi^{1/2})^{-1}\sum_j{}'\times[\exp(-Z^2R_j^2)+\tfrac{1}{2}\pi^{1/2}(ZR_j)^{-1}\operatorname{erfc}(ZR_j)], \quad \text{(B14)}$$

where[39]

$$\operatorname{erfc}(\zeta)=1-\operatorname{erf}(\zeta)=2\pi^{-1/2}\int_\zeta^\infty dt\exp(-t^2). \quad \text{(B15)}$$

[39] See Ref. 20, p. 297.

The other part of the sum Σ_3 may be rewritten with the Poisson sum formula[40]

$$\sum_j\exp(-\zeta^2R_j^2+i\mathbf{q}\cdot\mathbf{R}_j)=\zeta^{-2}n\pi\sum_l\exp[-(4\zeta^2)^{-1}(\mathbf{k}_l+\mathbf{q})^2], \quad \text{(B16)}$$

where $n=2/\sqrt{3}a^2$ is the density of lattice sites and $\{\mathbf{k}_l\}$ is the set of reciprocal lattice vectors associated with the direct lattice $\{\mathbf{R}_j\}$. Equation (B11) now becomes

$$\Sigma_3^{(1)}(\mathbf{q})=4\pi^{-1/2}\int_0^Z d\zeta\zeta^2\{\sum_j\exp(-\zeta^2R_j^2+i\mathbf{q}\cdot\mathbf{R}_j)-1\}$$
$$=4n\pi^{1/2}\int_0^Z d\zeta\sum_l\exp[-(4\zeta^2)^{-1}(\mathbf{k}_l+\mathbf{q})^2]-\tfrac{1}{3}4\pi^{-1/2}Z^3, \quad \text{(B17)}$$

where Eq. (B16) has been used explicitly. In the long-wavelength limit ($qa\ll1$), the ratio q/k_l is small and serves as an expansion parameter except in the single term $\mathbf{k}_l=0$. A rather lengthy calculation eventually yields

$$\Sigma_3^{(1)}(0)-\Sigma_3^{(1)}(\mathbf{q})=2n\pi q-n\pi^{1/2}q^2Z^{-1}+nq^2\sum_l{}'[\tfrac{1}{2}\pi k_l^{-1}\operatorname{erfc}(k_l/2Z)-\pi^{1/2}(2Z)^{-1}\exp(-k_l^2/4Z^2)]. \quad \text{(B18)}$$

The linear term in q reflects the long range of the interaction and arises from the term associated with the origin of the reciprocal lattice.

For a triangular array, typical direct and reciprocal reciprocal vectors are of the form $l\mathbf{a}_1+m\mathbf{a}_2$ and $l\mathbf{b}_1+m\mathbf{b}_2$, where l and m are integers and the fundamental lattice vectors are given by

$$\mathbf{a}_1=a\hat{x}, \qquad \mathbf{a}_2=\tfrac{1}{2}a(\hat{x}+\sqrt{3}\hat{y}),$$
$$\mathbf{b}_1=a^{-1}[\hat{x}-(\sqrt{3})^{-1}\hat{y}], \qquad \mathbf{b}_2=(2/a\sqrt{3})\hat{y}. \quad \text{(B19)}$$

The variables appearing in Eqs. (B14) and (B18) are ZR_j and $k_l/2Z$, respectively, which become identical if the constant Z is chosen as

$$Z=(n\pi)^{1/2}=(2\pi/\sqrt{3})^{1/2}a^{-1}. \quad \text{(B20)}$$

The remaining analysis is elementary, and we find

$$\eta_0=\tfrac{1}{2}n\bar{\kappa}\Lambda q+\bar{\eta}_0, \quad \text{(B21)}$$

where

$$\bar{\eta}_0=-(4\pi)^{-1}\bar{\kappa}\Lambda n^{1/2}q^2[1-\tfrac{1}{2}\pi^{1/2}\sum_{lm}{}'x_{lm}^{-1}\operatorname{erfc}(x_{lm})]. \quad \text{(B22)}$$

Here, the dimensionless quantity x_{lm} is defined as

$$x_{lm}=(2\pi/\sqrt{3})^{1/2}(l^2+lm+m^2)^{1/2}, \quad \text{(B23)}$$

[40] This is easily derived using the methods of Ref. 38.

and the sum in Eq. (B22) is over all positive and negative integers, omitting the single term $l=m=0$.

The calculation of $-\xi_0+i\alpha_0$ is only slightly more complicated than that given above, because the sixfold symmetry of the triangular lattice may again be used to simplify the explicit dependence on the polar angle χ. Detailed evaluation gives

$$-\xi_0+i\alpha_0=\tfrac{1}{2}n\bar{\kappa}\Lambda q\exp(2i\chi)+(-\bar{\xi}_0+i\bar{\alpha}_0), \qquad \text{(B24)}$$

where

$$-\bar{\xi}_0+i\bar{\alpha}_0=\tfrac{3}{2}\exp(2i\chi)\bar{\eta}_0. \qquad \text{(B25)}$$

In the derivation of Eq. (B25), it is necessary to use the following summation:

$$\sum_{lm}{}'(x_{lm}{}^2-\tfrac{1}{2})\exp(-x_{lm}{}^2)=\tfrac{1}{2}; \qquad \text{(B26)}$$

this equation may be proved from the Poisson sum formula Eq. (B16) evaluated for $\mathbf{q}=0$ by differentiating with respect to ζ^2 and then setting $\zeta^2=n\pi$.

Short-Range Contribution

In the preceding section, the function f_0 has been used to compute the long-range contribution to the lattice sums, including terms linear and quadratic in q. The corresponding short-range contribution will now be found with the function $\bar{f}$. Since $\bar{f}\sim r^{-5}$ as $r\rightarrow\infty$, the sums converge even when expanded to order q^2, and we may therefore write

$$\bar{\eta}=(16\pi)^{-1}\bar{\kappa}q^2\sum_j{}'\{-\tfrac{1}{2}\pi(R_j/\Lambda)^2 \times[\mathbf{H}_0(R_j/\Lambda)-Y_0(R_j/\Lambda)]+(R_j/\Lambda)-(\Lambda/R_j)\}, \qquad \text{(B27)}$$

$$-\bar{\xi}+i\bar{\alpha}=(32\pi)^{-1}\bar{\kappa}q^2\exp(2i\chi)\sum_j{}'\{\tfrac{1}{2}\pi(R_j/\Lambda)^2 \times[\mathbf{H}_{-2}(R_j/\Lambda)-Y_{-2}(R_j/\Lambda)]-3(\Lambda/R_j)\}. \qquad \text{(B28)}$$

The form of these expressions has been simplified by using both the recurrence relations for Struve and Neumann functions[20] and the triangular symmetry of the lattice. It is shown below that these sums do not affect the vibration frequencies in the limit of low vortex density ($a\gg\Lambda$), which occurs for $H_{c1}\lesssim H$. Hence, it is sufficient to evaluate Eqs. (B27) and (B28) in the intermediate-density limit ($r_c\ll a\ll\Lambda$) when $H_{c1}\ll H\ll H_{c2}$.

The fundamental identity to be used in computing both Eqs. (B27) and (B28) is the following integral representation[41]

$$\int_0^\infty\frac{x^\nu K_\nu(ax)\,dx}{x^2+z^2}=\frac{\pi^2z^{\nu-1}}{4\cos\nu\pi}[\mathbf{H}_{-\nu}(az)-Y_{-\nu}(az)], \qquad \text{(B29)}$$

valid for $\mathrm{Re}\,\nu>-\tfrac{1}{2}$. In particular, it can be shown that

$$-\tfrac{1}{2}\pi z^2[\mathbf{H}_0(z)-Y_0(z)]+z-z^{-1} =-2(\pi z)^{-1}\int_0^\infty dxK_0(x)x^4(x^2+z^2)^{-1}. \qquad \text{(B30)}$$

Equation (B27) may therefore be rewritten as

$$\bar{\eta}=-\bar{\kappa}q^2(8\pi^2\mu)^{-1}\int_0^\infty d\zeta\zeta^4(\zeta^2+\mu^2)^{-1} \times\{\sum_{lm}{}'(l^2+lm+m^2)K_0[\zeta(l^2+lm+m^2)^{1/2}]\}, \qquad \text{(B31)}$$

where $\mu=a/\Lambda$ is a small parameter. The summation in curly brackets was denoted by $\Sigma_{16}(\zeta)$ in I, Appendix B, where it was proved that

$$\sum_{lm}{}'(l^2+lm+m^2)K_0[\zeta(l^2+lm+m^2)^{1/2}] =(16\pi/\sqrt{3})\{\zeta^{-4}+\sum_{lm}{}'[(\zeta^2-\sigma^2)(\zeta^2+\sigma^2)^{-3}]\}. \qquad \text{(B32)}$$

Here, the abbreviation

$$\sigma^2=\tfrac{1}{3}16\pi^2(l^2+lm+m^2) =(8\pi/\sqrt{3})x_{lm}{}^2 \qquad \text{(B33)}$$

has been introduced. Substitution of Eq. (B32) into Eq. (B31) yields

$$\bar{\eta}=-\bar{\kappa}q^2(8\pi^2\mu)^{-1}\int_0^\infty d\zeta\zeta^4(\zeta^2+\mu^2)^{-1} \times(16\pi/\sqrt{3})\{\zeta^{-4}+\sum_{lm}{}'[(\zeta^2-\sigma^2)(\zeta^2+\sigma^2)^{-3}]\}. \qquad \text{(B34)}$$

The second sum Eq. (B28) may be treated similarly. The integral representation (B29) provides the identity

$$\tfrac{1}{2}\pi z^2[\mathbf{H}_{-2}(z)-Y_{-2}(z)]-3z^{-1} =-2(\pi z)^{-1}\int_0^\infty dxK_2(x)x^4(x^2+z^2)^{-1}, \qquad \text{(B35)}$$

which reduces Eq. (B28) to

$$(-\bar{\xi}+i\bar{\alpha})\exp(-2i\chi) =-\bar{\kappa}q^2(16\pi^2\mu)^{-1}\int_0^\infty d\zeta\zeta^4(\zeta^2+\mu^2)^{-1} \times\{\sum_{lm}{}'(l^2+lm+m^2)K_2[\zeta(l^2+lm+m^2)^{1/2}]\}. \qquad \text{(B36)}$$

The summation in curly brackets was also evaluated in I, Appendix B, where it was denoted $\Sigma_{26}(\zeta)$; the explicit result is

$$\sum_{lm}{}'(l^2+lm+m^2)K_2[\zeta(l^2+lm+m^2)^{1/2}] =(32\pi/\sqrt{3})\{\zeta^{-4}+\sum_{lm}{}'\zeta^2(\zeta^2+\sigma^2)^{-3}\}-2\zeta^{-2}, \qquad \text{(B37)}$$

[41] Reference 28, p. 426.

with σ defined in Eq. (B33). Substitution of Eq. (B37) into Eq. (B36) gives

$$(-\bar{\xi}+i\bar{\alpha})\exp(-2i\chi)=-\bar{\kappa}q^2(8\pi^2\mu)^{-1}\int_0^\infty d\zeta\zeta^4(\zeta^2+\mu^2)^{-1}$$
$$\times\{(16\pi/\sqrt{3})\zeta^{-4}-\zeta^{-2}+(16\pi/\sqrt{3})\zeta^2\sum_{lm}{}'(\zeta^2+\sigma^2)^{-3}\}. \quad \text{(B38)}$$

Equations (B34) and (B38) separately diverge like μ^{-2} for small μ; this singular behavior precisely cancels in the evaluation of the vibration frequency of the vortex lattice, which depends only on the quantity

$$\bar{\eta}+(\bar{\xi}-i\bar{\alpha})\exp(-2i\chi)=-(\bar{\kappa}q^2/8\pi^2\mu)J(\mu), \quad \text{(B39)}$$

where

$$J(\mu)\equiv\int_0^\infty d\zeta\zeta^4(\zeta^2+\mu^2)^{-1}$$
$$\times[\zeta^{-2}-(16\pi/\sqrt{3})\sum_{lm}{}'\sigma^2(\zeta^2+\sigma^2)^{-3}]. \quad \text{(B40)}$$

It is not difficult to see that the definite integral $J(\mu)$ is finite, because the summation over l and m behaves asymptotically like ζ^{-2} for large ζ and thus cancels the first term in square brackets. Furthermore, only the first two terms of the expansion in ascending powers of μ are required to evaluate the lattice vibrations. Nevertheless, direct expansion of Eq. (B40) in powers of μ^2 is clearly forbidden, and we must again resort to the Ewald method. Since

$$\zeta^{-2}=2\int_0^\infty d\rho\,\rho\exp(-\rho^2\zeta^2),$$

$$(\zeta^2+\sigma^2)^{-3}=\int_0^\infty d\rho\,\rho^5\exp[-\rho^2(\sigma^2+\zeta^2)], \quad \text{(B41)}$$

Eq. (B40) may be rewritten as

$$J(\mu)=J^{(1)}(\mu)+J^{(2)}(\mu), \quad \text{(B42)}$$

$$J^{(1)}(\mu)=\int_0^R\rho\,d\rho[2-(16\pi/\sqrt{3})\rho^4\sum_{lm}{}'\sigma^2\exp(-\rho^2\sigma^2)]$$
$$\times\int_0^\infty d\zeta\,\zeta^4(\zeta^2+\mu^2)^{-1}\exp(-\rho^2\zeta^2), \quad \text{(B43)}$$

$$J^{(2)}(\mu)=\int_0^\infty d\zeta\,\zeta^4(\zeta^2+\mu^2)^{-1}\int_R^\infty\rho\,d\rho\exp(-\rho^2\zeta^2)$$
$$\times[2-(16\pi/\sqrt{3})\rho^4\sum_{lm}{}'\sigma^2\exp(-\rho^2\sigma^2)]. \quad \text{(B44)}$$

The constant R will be chosen below to simplify the subsequent calculations.

In Eq. (B44), the integration over ρ may be performed directly, and we find

$$J^{(2)}(\mu)=\int_0^\infty d\zeta\,\zeta^4(\zeta^2+\mu^2)^{-1}\exp(-R^2\zeta^2)$$
$$\times\{\zeta^{-2}-(8\pi/\sqrt{3})\sum_{lm}{}'\sigma^2\exp(-R^2\sigma^2)[2(\zeta^2+\sigma^2)^{-3}$$
$$+2R^2(\zeta^2+\sigma^2)^{-2}+R^4(\zeta^2+\sigma^2)^{-1}]\}. \quad \text{(B45)}$$

Liberal use of partial fractions shows that Eq. (B45) depends only on a single definite integral and its derivatives

$$K(R^2,\mu^2)\equiv\int_0^\infty d\zeta\exp(-R^2\zeta^2)(\zeta^2+\mu^2)^{-1}. \quad \text{(B46)}$$

It is easy to verify that

$$-\partial K(R^2,\mu^2)/\partial R^2=(2R)^{-1}\pi^{1/2}-\mu^2K(R^2,\mu^2), \quad \text{(B47)}$$

which is an ordinary differential equation for K. An elementary integration yields

$$K(R^2,\mu^2)=(2\mu)^{-1}\pi\exp(\mu^2R^2)\,\text{erfc}(\mu R), \quad \text{(B48)}$$

where the complementary error function has been defined in Eq. (B15). A tedious calculation eventually gives

$$J^{(2)}(\mu)=(2R)^{-1}\pi^{1/2}-\tfrac{1}{2}\pi\mu$$
$$-(2\pi/\sqrt{3})\pi^{1/2}R\sum_{lm}{}'[\exp(-R^2\sigma^2)$$
$$+\tfrac{1}{2}\pi^{1/2}(\sigma R)^{-1}\,\text{erfc}(\sigma R)], \quad \text{(B49)}$$

where terms of order μ^2 have been neglected.

In contrast, the integrations in Eq. (B43) must be performed in the opposite order. The integral over ζ is obtained by differentiating Eq. (B46) twice, which shows that the leading term of Eq. (B43) is independent of μ and that the corrections are of order μ^2. Hence Eq. (B43) becomes

$$J^{(1)}(\mu)=\tfrac{1}{4}\pi^{1/2}\int_0^R\rho^{-2}\,d\rho$$
$$\times[2-(16\pi/\sqrt{3})\rho^4\sum_{lm}{}'\sigma^2\exp(-\sigma^2\rho^2)]+O(\mu^2). \quad \text{(B50)}$$

The sum over lattice sites may be rewritten with the Poisson sum formula; it is not difficult to show from Eq. (B16) that

$$2-(16\pi/\sqrt{3})\rho^4\sum_{lm}{}'\sigma^2\exp(-\sigma^2\rho^2)$$
$$=-2\sum_{lm}{}'[1-(g^2/4\rho^2)]\exp(-g^2/4\rho^2), \quad \text{(B51)}$$

where

$$g^2=l^2+lm+m^2. \quad \text{(B52)}$$

The remaining integration is elementary, and we find

$$J^{(1)}=(4R)^{-1}\pi^{1/2}\sum_{lm}{}'\{\exp(-g^2/4R^2)-\tfrac{1}{2}\pi^{1/2}(g/2R)^{-1}\operatorname{erfc}(g/2R)\}. \quad (B53)$$

If R is chosen as

$$R=\tfrac{1}{2}(\sqrt{3}/2\pi)^{1/2}, \quad (B54)$$

then both $J^{(1)}$ and $J^{(2)}$ contain the same lattice sums, and the definite integral $J(\mu)$ therefore reduces to

$$J(\mu)=\pi(2/\sqrt{3})^{1/2}[1-\tfrac{1}{2}\pi^{1/2}\sum_{lm}{}' x_{lm}^{-1}\operatorname{erfc}(x_{lm})]-\tfrac{1}{2}\pi\mu+O(\mu^2). \quad (B55)$$

A combination of Eqs. (B39) and (B55) yields

$$\bar{\eta}+(\bar{\xi}-i\bar{\alpha})\exp(-2i\chi)=-\bar{\kappa}q^2(8\pi\mu)^{-1}(2/\sqrt{3})^{1/2}\times[1-\tfrac{1}{2}\pi^{1/2}\sum_{lm}{}' x_{lm}^{-1}\operatorname{erfc}(x_{lm})]+\bar{\kappa}q^2(16\pi)^{-1}. \quad (B56)$$

Evaluation of Vibration Frequencies

All of the quantities required for evaluating the vibration frequencies ω have now been computed. The explicit expression from Sec. V

$$\omega^2=\eta^2-(\alpha^2+\xi^2) \quad (B57)$$

may be separated into contributions from the long- and short-range parts of the interaction

$$\omega^2=(\eta_0+\bar{\eta})^2-(\alpha_0+\bar{\alpha})^2-(\xi_0+\bar{\xi})^2. \quad (B58)$$

Different analysis is required for the low-density ($\mu\gg 1$) and intermediate-density ($\mu\ll 1$) lattice, and we shall first consider the case $\mu\gg 1$. Equations (B22) and (B24) show that the quadratic terms in q arising from f_0 are of order μ^{-1} for all μ. In contrast, the corresponding quadratic terms arising from $\bar{f}$ exhibit a more complicated dependence on μ. For $\mu\gg 1$, the distance between vortices a is large compared with the effective penetration depth Λ, and both Eqs. (B27) and (B28) may be expanded in powers of R_j/Λ; the asymptotic form of the Struve and Neumann functions shows that $\bar{\eta}$ and $\bar{\xi}-i\bar{\alpha}$ are each of order μ^{-3} and therefore negligible in comparison with the leading term of order μ^{-1}. This result is physically obvious, because only the asymptotic tail of the interaction can affect the long-wavelength dispersion relation in the low-density limit. Thus, Eq. (B58) reduces to

$$\omega^2=\eta_0^2-\alpha_0^2-\xi_0^2 \qquad (\mu\gg 1) \quad (B59)$$

and substitution of Eqs. (B21)–(B25) yields

$$\omega^2=(\tfrac{1}{4}n\bar{\kappa})^2q^3\Lambda^2(n\pi)^{-1/2}C \qquad (\mu\gg 1), \quad (B60)$$

where

$$C=2\pi^{-1/2}-\sum_{lm}{}' x_{lm}^{-1}\operatorname{erfc}(x_{lm})\approx 1.10611, \quad (B61)$$

and the relation $n=2/\sqrt{3}a^2$ has been used. The sum in Eq. (B61) converges very rapidly, and only the first few neighbors need be included.

In the opposite limit ($\mu\ll 1$), the continuum approximation Eq. (38) suggests that ω is of order $n\bar{\kappa}q^{3/2}\Lambda^{1/2}a$; this means that the singular μ^{-1} dependence of the long-range lattice sums [Eqs. (B22) and (B24)] must be exactly cancelled by a similar behavior of the short-range sums [Eq. (B56)]. Such a cancellation in fact occurs, although we have been unable to prove this except by the detailed calculations discussed above. The remaining analysis is straightforward and gives

$$\omega^2=(\tfrac{1}{4}n\bar{\kappa})^2q^3\Lambda(n\pi)^{-1} \qquad (\mu\ll 1). \quad (B62)$$

Thus the triangular lattice is stable against small perturbation both in the limit of low densities ($\mu\gg 1$) and intermediate densities ($\mu\ll 1$); this conclusion presumably remains valid for intermediate values of μ.